

Coherent spin dynamics in quantum wells in quantizing magnetic field

E. Ya. Sherman and J.E. Sipe¹

¹*Department of Physics and Institute for Optical Sciences,
University of Toronto, 60 St. George Street,
Toronto, Ontario, Canada M5S 1A7*

Abstract

We investigate theoretically the coherent longitudinal and transversal spin relaxation of photoexcited electrons in quantum wells in quantized magnetic fields. We find the relaxation time for typical quantum well parameters between 10^2 and 10^3 ps. For a realistic random potential the relaxation process depends on the electron energy and g -factor, demonstrating oscillations in the spin polarization accompanying the spin relaxation. The dependence of spin relaxation on applied field, and thus on the corresponding "magnetic" length, can be used to characterize the spatial scale of disorder in quantum wells.

I. INTRODUCTION

A magnetic field applied to a two-dimensional (2D) electron system changes both the orbital and spin dynamics of the carriers. A crucial aspect of this dynamics is spin relaxation, which arises due to spin-orbit (SO) coupling. This coupling is well-described in zincblende (001)-grown structures by a Hamiltonian H_{SO} that is the sum of two terms, a Rashba Hamiltonian^{1,2} $H_{\text{R}} = \alpha_{\text{R}}(\sigma_x p_y - \sigma_y p_x)/\hbar$ and a Dresselhaus Hamiltonian^{3,4} $H_{\text{D}} = \alpha_{\text{D}}(\sigma_x p_x - \sigma_y p_y)/\hbar$, where α_{R} and α_{D} are coupling constants, σ are the Pauli matrices, and $\mathbf{p}_{\parallel} = (p_x, p_y) = -i\hbar\nabla_{\parallel} - (e/c)\mathbf{A}_{\parallel}$. Here e is the electron charge, and \mathbf{A}_{\parallel} is a vector-potential of the external field; H_{R} and H_{D} arise, respectively, due to the artificial macroscopic asymmetry of the structure, and due to the microscopic inversion asymmetry of the zincblende unit cell. The coupling constants α_{R} and α_{D} typically range from 10^{-10} to 10^{-9} eVcm.⁵

The spin relaxation of conducting electrons is usually described using a Dyakonov-Perel'⁶ approach, where it is assumed that the orientation of the spin precession axis changes randomly through scattering by impurities. In the absence of an external magnetic field the spin relaxation rate is $\gamma_{\text{DP}} \approx (\alpha/\hbar)^2 p^2 \tau$, with τ the momentum relaxation time, and where α depends on α_{R} and α_{D} . Since spin relaxation arises due to the random spatial motion of the electron, the orbital effect of a magnetic field, which can restrict the region over which an electron can sample the effect of impurities, influences the spin relaxation. At $\omega_c \tau \gg 1$, the relaxation rate decreases by a factor⁷ of $\omega_c^2 \tau^2$, where $\omega_c = |e|B/mc$ is the cyclotron frequency for a magnetic field B , with m being the electron effective mass. In such a strong field the electron path becomes close to a circle, with scattering effects negligible. On this orbit the mean spin precession angle vanishes due to the fact that the electron velocity $\mathbf{v}_{\parallel}(t + \pi/\omega_c) = -\mathbf{v}_{\parallel}(t)$, and, therefore, the randomness in the precession is suppressed. For a random SO coupling a non-quantizing magnetic field can, however, speed up spin relaxation and make the relaxation process Gaussian rather than exponential in its time dependence.⁸ The B -dependence of the relaxation rate in nonquantizing fields can demonstrate magnetoquantum oscillations, as shown by self-consistent Born approximation for 2D electron gas in a short-range potential of impurities.⁹ Analysis of spin relaxation in weak magnetic fields allows the extraction of SO coupling parameters from experimental data.¹⁰

Studies of spin dynamics of itinerant electrons typically assume that their motion can be described semiclassically. However, spin dynamics of carriers with quantized lateral motion is of interest both for understanding of the fundamental physics of spin transport¹¹ and for applications of nanosize systems in spintronics. An interesting example of a system with quantum lateral motion is 2D electron gas in a strong magnetic field, where Landau states must be used to represent the electrons and only a few (or a fraction) of the Landau levels is occupied. An analogous regime has been widely discussed for quantum dots, where electrons are confined by an external potential. There the SO coupling mixes states with opposite spins, making spin-flip transitions accompanied by phonon emission possible.¹² Here we are interested in itinerant two-dimensional electrons, where early experimental data has shown the suppression of spin relaxation in strong magnetic fields.¹³ The treatment of 2D electrons in quantizing fields is rather subtle,¹⁴ with different theoretical techniques giving

different results even for static properties such as the density of states. The analytical approaches require approximations that might be not widely applicable. The situation becomes even more complicated for the response functions, such as those describing charge and spin currents, as well as relaxation processes. An analytical study by Bastard¹⁵ of spin relaxation in the self-consistent Born approximation, for a short-range random potential and a small electron g -factor, where the Zeeman splitting is small in comparison with the level broadening, showed that both spin-orbit coupling and disorder play a role, and allowed an estimation of the relaxation rate.

Here we perform a numerical study of the problem using the exact diagonalization technique for a large but finite-size system, and show the diverse physical mechanisms that contribute to the relaxation process. This approach has proven its applicability in calculations of the spin-Hall conductivity of a disordered 2D electron gas,¹⁶ where the spectrum and the full set of eigenstates are required for the calculation.

II. MODEL OF DISORDER AND SPIN DYNAMICS

We consider a quantum well in a magnetic field parallel to the growth direction, $\mathbf{B} = B\hat{z}$. The field forms spin-split Landau levels, inhomogeneously broadened by the disorder. In undoped quantum wells the random potential arises due to the monolayer islands of the parent compounds at the interfaces (thickness fluctuations) and due to the content variations near the interfaces.^{18–20} The island patterns depend on the growth conditions. The Hamiltonian for an electron in an undoped quantum well with disorder is

$$H = \frac{p_{\parallel}^2}{2m} + \mu_B g (\boldsymbol{\sigma} \cdot \mathbf{B})/2 + H_{\text{SO}}(\boldsymbol{\sigma}, \mathbf{p}_{\parallel}) + U(\boldsymbol{\rho}), \quad (1)$$

where the random contribution $U(\boldsymbol{\rho}) = \sum_d V(\boldsymbol{\rho} - \mathbf{R}_d)$, where \mathbf{R}_d is the position of a defect. As a model, we consider the Gaussian potential $V(\boldsymbol{\rho}) = V_r \exp(-\rho^2/R_g^2)$ with the areal density of defects $N(\boldsymbol{\rho}) = \sum_d \delta(\boldsymbol{\rho} - \mathbf{R}_d)$, and a correlation function $\langle N(\mathbf{0}) N(\boldsymbol{\rho}) \rangle = N_{\text{imp}} \delta(\boldsymbol{\rho})$, where N_{imp} is the average areal density of defects. To avoid the uniform shift of the Landau levels, we assume that $V_r = \pm V_g$ varies from site to site, being either positive or negative such that the mean value $\langle U(\boldsymbol{\rho}) \rangle = 0$. The correlation function of the random potential is $\langle U(\mathbf{0}) U(\boldsymbol{\rho}) \rangle \equiv \langle U^2 \rangle F_c(\rho)$, where²¹

$$\langle U^2 \rangle = \frac{\pi}{2} N_{\text{imp}} R_g^2 V_g^2, \quad F_c(\rho) = e^{-\rho^2/2R_g^2}. \quad (2)$$

At $B = 0$ the momentum relaxation time in this model is given by:

$$\frac{1}{\tau} = N_{\text{imp}} V_g^2 R_g \frac{m}{\hbar^3} \begin{cases} 2\pi^2 R_g^3, & \lambda \gg R_g, \\ \lambda^3/16\sqrt{2}\pi^3, & R_g \gg \lambda, \end{cases} \quad (3)$$

where $\lambda = 2\pi/k$ is the electron wavelength. The result for the $\lambda \gg R_g$ case is valid in the Born approximation for scattering by well-separated impurities,¹⁴ in the opposite limit the

electron is moving semiclassically in a smooth potential, where $\tau \propto \lambda^{-3}$ depends on the electron energy.²²

To describe the magnetic field, we choose the Landau gauge $\mathbf{A} = (0, Bx, 0)$ where the eigenstates $|nKs\rangle$ of the unperturbed Hamiltonian $p_{\parallel}^2/2m + \mu_B g(\boldsymbol{\sigma} \cdot \mathbf{B})/2$ are represented by the spinors:

$$\phi_{nKs}(\boldsymbol{\rho}) = \frac{e^{ik_y y}}{\sqrt{L_y}} \frac{1}{\pi^{1/4} \sqrt{2^n n! l_B}} \exp\left[-\frac{x_K^2}{2l_B^2}\right] H_n\left(\frac{x_K}{l_B}\right) \beta_s, \quad (4)$$

where β_s is the spinor corresponding to one of the states $|s\rangle = |\uparrow\rangle, |\downarrow\rangle$, n is the Landau level number, the magnetic length $l_B = \sqrt{\hbar c/|e|B}$, $x_K \equiv x - X_K$, $X_K = -k_y l_B^2$ is the center of the oscillator wavefunction, $k_y = -2\pi K/L_y$, $K = 0, 1, \dots, K_{\max}$, L_y is the y -axis size of the system and H_n is the n th Hermite polynomial. The corresponding unperturbed spectrum is $E(n, s) = \hbar\omega_c(n + 1/2) \pm g\mu_B B/2$. Due to the selection rules for the matrix elements of \mathbf{p}_{\parallel} and spin components σ_x and σ_y , the SO coupling only connects states of opposite spins from nearest Landau levels.²³ This results in a small shift in the energies of the order of $m(\alpha/\hbar)^2$. The matrix elements of the disorder Hamiltonian diagonal over the spin index are given by:

$$H_{\text{rnd}}(n'K's'; nKs) = \int d^2\rho \bar{\phi}_{n'K's'}(\boldsymbol{\rho}) U(\boldsymbol{\rho}) \phi_{nKs}(\boldsymbol{\rho}), \quad (5)$$

and couple states in all Landau levels for which $|X_K - X_{K'}| \lesssim l_B$, and, correspondingly $|k_y - k'_y| \lesssim 1/l_B$, thus leading to electron localization both in the x - and y -directions. As a result the density of eigenstates with energies E_j has the form of broadened Landau levels, typically (at $B = 5$ T) with the width Γ on the order of or less than 1 meV, at least an order of magnitude smaller than $\hbar\omega_c$. The corresponding eigenfunctions are expressed as linear combinations:

$$|\psi_j\rangle = \sum_{n,K,s} a_{nKs}^{(j)} |nKs\rangle, \quad (6)$$

with complex coefficients $a_{nKs}^{(j)}$. Only a few of the amplitudes $a_{nKs}^{(j)}$ are nonnegligible, since $U(\boldsymbol{\rho})$ couples only the states with close momenta k_y . Due to the combined effect of disorder and SO coupling, the $|nK_1 \uparrow\rangle$ and $|nK_2 \downarrow\rangle$ states within one Landau level become coupled as shown in Fig. 1(a), thus introducing randomness in the spin precession at the frequency scale Γ/\hbar , and, in turn, spin relaxation.

We consider an electron-hole plasma injected by a light pulse in an undoped quantum well (Fig.1(b)). We assume that the plasma density is small, and neglect all many-body effects. Alternatively, for a doped quantum well, we assume the carriers are injected into unoccupied Landau states above the Fermi level. We concentrate on the spin relaxation of electrons, since the hole spins relax much faster.²⁴

We assume that the spectral width of the exciting light $\Delta\omega$ satisfies the conditions $\Gamma \ll \hbar\Delta\omega \ll \hbar\omega_c$ as shown in Fig.1(b). Therefore, the states $|\psi_i^{\text{in}}(t=0)\rangle$ (index $1 \leq i \leq N_{\text{in}}$ numerates the injected electrons, with their total number being N_{in}) in which the electrons are injected can be written as superposition of the $|nK_i s\rangle$ states from essentially one Landau level n_{in} and spin projection s_{in} determined by the light polarization.²⁵ Within

this approximation a unitary transformation connects the full sets of $|\psi_i^{\text{in}}(t=0)\rangle$ and $|n_{\text{in}}K_i s_{\text{in}}\rangle \equiv |\Phi_{K_i}(t=0)\rangle$ states. Thus, in place of averaging the time-dependent spin components over $|\psi_i^{\text{in}}(t)\rangle$, we can average over the $|\Phi_{K_i}(t)\rangle$ as follows:

$$\begin{aligned}\langle\sigma_\zeta(t)\rangle &= \frac{1}{N_{\text{in}}} \sum_{i=1}^{N_{\text{in}}} \langle\psi_i^{\text{in}}(t)| \sigma_\zeta |\psi_i^{\text{in}}(t)\rangle \\ &= \frac{1}{N_{\text{in}}} \sum_{i=1}^{N_{\text{in}}} \langle\psi_i^{\text{in}}(t=0)| e^{iHt/\hbar} \sigma_\zeta e^{-iHt/\hbar} |\psi_i^{\text{in}}(t=0)\rangle \\ &= \frac{1}{N_{\text{in}}} \sum_{i=1}^{N_{\text{in}}} \langle\Phi_{K_i}^{\text{in}}(t)| \sigma_\zeta |\Phi_{K_i}^{\text{in}}(t)\rangle.\end{aligned}\tag{7}$$

This relaxation is coherent in the sense that the total energy $\langle H \rangle$ of the injected electrons is conserved on the timescale considered here and is not transformed into lattice phonons or low-energy electron excitations.

To evaluate $\langle\sigma_\zeta(t)\rangle$ numerically, we have to find the spinor representation of the $|\Phi_{K_i}^{\text{in}}(t)\rangle$; that is, we must determine the eigenstates of the Hamiltonian H in Eq.(1). To do this, we have chosen a basis of $n_B = 256$ states per Landau level for each spin projection. The total Hilbert space included $N_L = 6$ Landau levels, which we find sufficient for our choice of the parameters given below, for which $\hbar\omega_c \gg \Gamma$. The coefficients a_{nKs}^j considered as the elements of the eigenvectors are arranged in the following order: $(\{a_{0K\uparrow}\}, \{a_{0K\downarrow}\}, \dots, \{a_{N_L-1K\uparrow}\}, \{a_{N_L-1K\downarrow}\})$, where in every subset K is running from 0 to K_{max} .

III. NUMERICAL RESULTS: THE ROLE OF THE g -FACTOR AND THE DISORDER LANDSCAPE

For sample calculation we consider two types of typical structures. The first is a symmetric quantum well with electrons located in a GaAs layer, with the Dresselhaus SO coupling $\alpha_D = 0.35 \times 10^{-9}$ eVcm, $m = 0.067m_0$ (m_0 is the free electron mass), and $g = -0.45$. The other is an asymmetric structure with the electrons located in a $\text{In}_{0.5}\text{Ga}_{0.5}\text{As}$ layer, with¹⁷ a Rashba SO coupling $\alpha_R = 0.35 \times 10^{-9}$ eVcm, $m = 0.05m_0$, and $g = 4$. We assume that both of them have a width of 10 nm. For these structures the ratio of effective masses $m(\text{GaAs})/m(\text{In}_{0.5}\text{Ga}_{0.5}\text{As}) = 1.35$, while the electron g -factors are different approximately by a factor of $|g(\text{In}_{0.5}\text{Ga}_{0.5}\text{As})/g(\text{GaAs})| = 8.9$. It is the difference in g -factors that will lead to large quantitative difference between the spin relaxation in these two structures.

As a realization of the disorder¹⁹ we consider a short-range potential with $V_g = 3.5$ meV for GaAs and $V_g = 5.0$ meV for $\text{In}_{0.5}\text{Ga}_{0.5}\text{As}$ structure, $R_g = 3$ nm, and $N_{\text{imp}} = 10^{12}$ cm⁻². These parameters can describe the random potential arising due to the single unit cell layer thickness variations in quantum wells of the width of 10 nm. Since $l_B \gg R_g$, the width of the Landau level $\Gamma = \hbar\sqrt{2\omega_c/\pi\tau}$ does not depend on the level number. We also consider a long-range potential with $R_g = 20$ nm and the same amplitudes V_g as for the short-range one. Both these random potentials lead to mobilities of $\approx 5 \times 10^4$ cm²/Vs at concentrations

of electrons $N_{\text{el}} \approx 5 \times 10^{11} \text{ cm}^{-2}$ in both structures. Note that in the case of a long-range potential $R_g \gg l_B$, we have $\Gamma = 2\sqrt{\langle U^2 \rangle}$. This spatial scale can be achieved by quantum well fabrication with growth interruption¹⁸, or by remote doping on the quantum well sides.

The results of numerical calculations for the GaAs quantum well are presented in Figs. 2 and 3 for different initial spin components $\langle \sigma_z(0) \rangle = -1$ and $\langle \sigma_x(0) \rangle = 1$, respectively, two different types of disorder, and magnetic fields of 4 T and 8 T. In these GaAs-based structures we find the relaxation times on the order of 100 ps, of the same order of magnitude for out-of-plane $\langle \sigma_z(t) \rangle$ and in-plane $\langle \sigma_x(t) \rangle$ spin components. They relax on the same time scale since the same mechanism, that is the random spin precession, leads to the relaxation in both spin polarizations. With the increase of the Landau level number, the electron motion becomes less sensitive to the disorder, and the spin relaxation time increases, as demonstrated by the results for $n = 2$ in Fig. 2 and Fig.3. This corresponds well to the experimental results of Sih *et al.*²⁶ Spin relaxation due to acoustic phonon emission²⁷ occurs at a much longer time scale, and is not considered here. An interesting effect is the spin precession in the $\langle \sigma_z(t) \rangle$ relaxation, clearly seen in our calculations. The spin-orbit interaction couples Zeeman-split Landau levels which are broadened due to disorder, and so the z -component of the spin is not a constant of motion. For this reason, the initially prepared $\sigma_z = \pm 1$ states precess with the frequencies in the range determined by the Zeeman splitting and the Landau level width, distributed over interval of the width Γ/\hbar centered at $g\mu_B B/\hbar$. The precession amplitude is smeared with time due to spin relaxation, as seen in our results.

Fig. 4 presents the results for $\text{In}_{0.5}\text{Ga}_{0.5}\text{As}$ structure, where the spin relaxation is much slower. Due to the increased Zeeman splitting the frequency of the spin oscillations here is considerably larger than that in the GaAs quantum well, and the oscillations become more well-defined. The role of the Zeeman splitting $|g|\mu_B B$ in spin relaxation, clearly seen when one compares the results for the GaAs and $\text{In}_{0.5}\text{Ga}_{0.5}\text{As}$ structures, is crucial to the mechanism of the spin relaxation, and can be understood as follows.²⁸ The random potential accompanied by SO coupling leads to the spin-flip transitions. However, only spatially close states (with a large overlap) with opposite spins can contribute effectively to the spin relaxation. On the other hand, the spin-flip process should conserve energy, and, therefore, a lateral distance ℓ_s on which the orbital has to be displaced to find its spin-flip partner state depends on the Zeeman splitting. To understand the effect we evaluate the fluctuation of the expectation value of energy for a state described by wave function $\psi(\boldsymbol{\rho})$:

$$\begin{aligned} \langle (\Delta U_{\boldsymbol{\rho}})^2 \rangle &= \left\langle \left[\int U(\boldsymbol{\rho}_1) (\psi^2(\boldsymbol{\rho}_1) - \psi^2(\boldsymbol{\rho}_1 + \boldsymbol{\rho})) d^2 \rho_1 \right]^2 \right\rangle \\ &= 2\langle U^2 \rangle \int F_c(\boldsymbol{\rho}_1 - \boldsymbol{\rho}_2) \psi^2(\boldsymbol{\rho}_1) [\psi^2(\boldsymbol{\rho}_2) - \psi^2(\boldsymbol{\rho}_2 + \boldsymbol{\rho})] d^2 \rho_1 d^2 \rho_2. \end{aligned} \quad (8)$$

This fluctuation can be calculated in two limiting cases as:

$$\langle (\Delta U_{\boldsymbol{\rho}})^2 \rangle = 2\langle U^2 \rangle \begin{cases} 1 - F_c(\rho), & l_B \ll R_g, \\ \frac{R_g^2}{l_B^2} \left[1 - e^{-\rho^2/4l_B^2} \right], & l_B \gg R_g, \end{cases} \quad (9)$$

where we assumed for an estimate that for the ground orbital state $\psi^2(\boldsymbol{\rho}) = \exp(-\rho^2/2l_B^2)/2\pi l_B^2$. If ℓ_s determined by energy conservation is less than l_B , that is $|g|\mu_B B \leq \langle U^2 \rangle^{1/2} \min(l_B/R_g, R_g/l_B)$, the relaxation occurs effectively. In the opposite case, the decay time increases due to a small spatial overlap of the initial and final states. In other words, if $|g|\mu_B B > \Gamma$, the spin relaxation is suppressed, since the energy conservation cannot be fulfilled in the spin-flip process. In this case the z -component of spin relaxes from the initial value by approximately $\Gamma/|g|\mu_B B$, and then the system has to pass by emitting acoustic phonons through a phonon bottleneck²⁷ for the spin to relax it further.

This "spin-flip distance" argument explains the difference between the spin relaxation for a "long" and "short"- range potentials shown in Fig. 4. In both cases the amplitude of the potential fluctuations is the same, but in the case of a long-range potential the electron must be displaced a longer distance to find its spin-flip partner state. Thus, the relaxation rate decreases with the increase of the correlation length R_g , in agreement with results presented in Fig.4.

IV. CONCLUSIONS AND POSSIBLE APPLICATIONS

To conclude, we investigated the spin relaxation in quantizing magnetic fields in a disordered 2D electron gas, and found that the result depends on the Landau level number, and that the process is accompanied by spin oscillations. The mechanism discussed here is different from the usual Dyakonov-Perel' mechanism, and is closer in nature to the Elliot-Yafet mechanism, in which the spin relaxation rate increases with the disorder.⁴ The relaxation rate depends on the details of the potential and electron g -factor, and cannot be understood solely in terms of the electron mobility.

The results obtained can be used to characterize the disorder in undoped quantum wells. Such disorder is typically probed experimentally by studying the inhomogeneous broadening of the spectra of excitons, a technique restricted either to the spatial scale given by the exciton Bohr radius or by the exciton localization length.²⁰ Neither of these lengths can be changed externally in a well-controlled way. The advantage of studying the spin relaxation in a magnetic field is that it allows probing different spatial scales of disorder by controllably changing the length l_B trough varying the magnetic field.

Acknowledgment. We are grateful to H.M. van Driel, M.E. Flatté, A. Najmaie, K. Nomura, J. Prineas, J. Sinova, and A. Smirl for valuable discussions, and to P. Chak and F. Nastos for help in numerical calculations. This work was supported by the DARPA SpinS program and by the FWF grant P15220.

-
- ¹ Yu. A. Bychkov and E. I. Rashba, JETP Lett. **39**, 79 (1984), E.I. Rashba, Sov. Phys. - Solid State **2**, 1874, (1964)
 - ² E.I. Rashba, Sov. Phys. - Solid State **2**, 1109 (1960) (Fizika Tverdogo Tela **2**, 1224 (1960))
 - ³ M.I. Dyakonov and V.Yu. Kachorovskii, Sov. Phys. Semicond. **20**, 110 (1986) For holes: E.I. Rashba and E.Ya. Sherman, Phys. Lett. **A 129**, 175 (1988), O. Mauritz and U. Ekenberg, Phys. Rev. **B 60**, R8505 (1999), R. Winkler, S.J. Papadakis, E.P. De Poortere, and M. Shayegan, Phys. Rev. Lett., **85**, 4574 (2000).
 - ⁴ A comprehensive review can be found in: I. Zutíć, J. Fabian and S. Das Sarma, Rev. Mod. Phys. **76**, 323 (2004)
 - ⁵ D. Stein, K. v. Klitzing, and G. Wiemann, Phys. Rev. Lett. **51**, 130 (1983); B. Jusserand, D. Richards, G. Allan, C. Priester, and B. Etienne, Phys. Rev. **B 51**, 4707 (1995); W. Knap, C. Skierbiszewski, A. Zduniak, E.Litwin-Staszewska, D. Bertho, F. Kobbi, and J. L. Robert, G. E. Pikus, F. G. Pikus, S. V. Iordanskii, V. Mosser, K. Zekentes, Yu. B. Lyanda-Geller, Phys. Rev. **B 53**, 3912 (1996); J. Nitta, T. Akazaki, H. Takayanagi, and T. Enoki, Phys. Rev. Lett. **78**, 1335 (1997); D. Grundler, Phys. Rev. Lett. **84**, 6074 (2000); T. Koga, J. Nitta, T. Akazaki, and H. Takayanagi, Phys. Rev. Lett. **89**, 046801 (2002); J. B. Miller, D. M. Zumbühl, C. M. Marcus, Y. B. Lyanda-Geller, D. Goldhaber-Gordon, K. Campman, and A. C. Gossard, Phys. Rev. Lett. **90**, 076807 (2003); O. Z. Karimov, G. H. John, R. T. Harley, W. H. Lau, M. E. Flatté, M. Henini, and R. Airey, Phys. Rev. Lett. **91**, 246601 (2003)
 - ⁶ M.I. Dyakonov and V.I. Perel', Sov. Phys. -Solid State **13**, 3023 (1972)
 - ⁷ E.L. Ivchenko, Fiz. Tverd. Tela **15**, 1566 (1973) [Sov. Phys. Solid State **15**, 1048 (1973)].
 - ⁸ M.M. Glazov and E.Ya. Sherman, Phys. Rev. **B 71**, 241312(R) (2005), L. E. Golub and E. L. Ivchenko, Phys. Rev. **B 69**, 115333 (2004)
 - ⁹ A. A. Burkov and L. Balents, Phys. Rev. **B 69**, 245312 (2004)
 - ¹⁰ M. M. Glazov, Phys. Rev. **B 70**, 195314 (2004), Z. Wilamowski and W. Jantsch, Phys. Rev. **B 69**, 035328 (2004)
 - ¹¹ See, for example: F. Mireles and G. Kirczenow, Europhys. Lett. **59**, 107 (2002)
 - ¹² A. V. Khaetskii and Y. V. Nazarov, Phys. Rev. **B 61**, 12639 (2000), and Phys. Rev. **B 64**, 125316 (2001); J.L. Cheng, M.W. Wu, and C.Lu, Phys. Rev. **B 69**, 115318 (2004); M. Florescu, S. Dickman, M. Ciorga, A. Sachrajda, and P. Hawrylak, Physica E **22**, 414 (2004).
 - ¹³ M. Potemski, J. C. Maan, A. Fasolino, K. Ploog, and G. Weimann Phys. Rev. Lett. **63**, 2409 (1989)
 - ¹⁴ T. Ando, A.B. Fowler, and F. Stern, Rev. Mod. Phys. **54**, 437 (1982), K. Esfarjani, H. R. Glyde, and V. Sayakanit, Phys. Rev. **B 41**, 1042 (1990), M. Nithisoontorn, R. Lassnig, and E. Gornik, Phys. Rev. **B 36**, 6225 (1987)
 - ¹⁵ G. Bastard, Phys. Rev. **B 46**, 4253 (1992)
 - ¹⁶ K. Nomura, J. Sinova, T. Jungwirth, Q. Niu, and A. H. MacDonald, Phys. Rev. **B 71**, 041304(R) (2005), K. Nomura, J. Sinova, N. A. Sinitsyn, and A. H. MacDonald Phys. Rev. **B 72**, 165316 (2005)

- ¹⁷ See, e.g. work of Nitta *et al.* in Ref.[5].
- ¹⁸ K. Leosson, J. R. Jensen, W. Langbein, and J. M. Hvam, Phys. Rev. B **61**, 10322 (2000)
- ¹⁹ A. Patanè, A. Polimeni, and M. Capizzi, F. Martelli, Phys. Rev. B **52**, 2784 (1995)
- ²⁰ H. Castella, J. W. Wilkins, Phys. Rev. B **58**, 16186 (1998)
- ²¹ A.L. Efros and B.I. Shklovskii, *Electronic Properties of Doped Semiconductors*, Springer, Heidelberg (1989)
- ²² A. D. Mirlin, J. Wilke, F. Evers, D. G. Polyakov, and P. Wölfle Phys. Rev. Lett. **83**, 2801 (1999)
- ²³ J. Schliemann, J. C. Egues, and D. Loss, Phys. Rev. B **67**, 085302 (2003)
- ²⁴ D. J. Hilton and C. L. Tang, Phys. Rev. Lett. **89**, 146601 (2002)
- ²⁵ S. Pfalz, R. Winkler, T. Nowitzki, D. Reuter, A. D. Wieck, D. Hägele, and M. Oestreich, Phys. Rev. B **71**, 165305 (2005)
- ²⁶ V. Sih, W. H. Lau, R. C. Myers, A. C. Gossard, M. E. Flatté, and D. D. Awschalom, Phys. Rev. B **70**, 161313(R) (2004)
- ²⁷ D. M. Frenkel, Phys. Rev. B **43**, 14228 (1991)
- ²⁸ We mention that a model calculation with $m = 0.05m_0$ and $g = 0.45$ shows the results similar to those in Fig.2 but different from Fig.4.

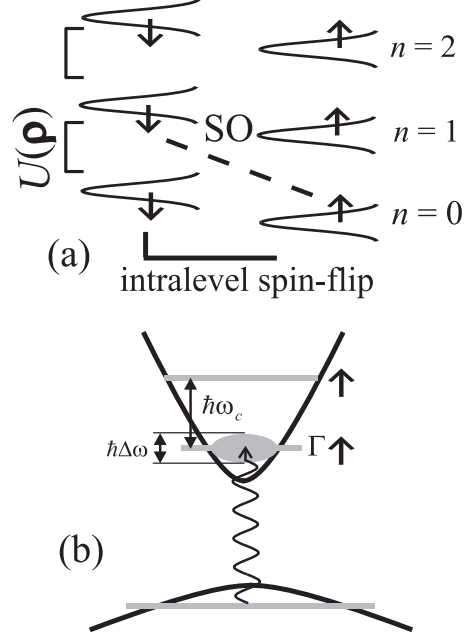


FIG. 1: (a) Schematic plot of the broadened Landau levels and interlevel transitions for $\alpha_R = 0, \alpha_D \neq 0$. Arrows label electron spins, and the index n corresponds to the Landau level number. (b) Schematic plot of the optical transitions between the Landau levels. Only one spin projection is presented.

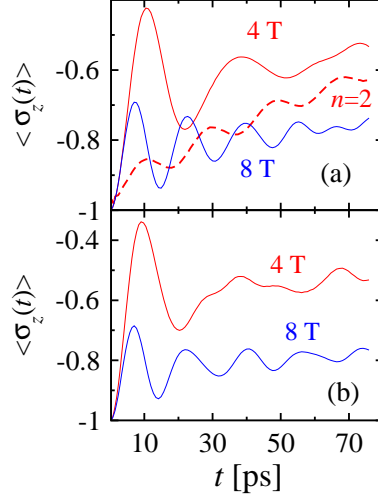


FIG. 2: (Color online) (a) $\langle \sigma_z(t) \rangle$ for a short-range ($R_g = 3$ nm) potential, and (b) $\langle \sigma_z(t) \rangle$ for a long-range ($R_g = 20$ nm) potential in the GaAs quantum well. Solid lines correspond to $n = 0$; the dashed line in Fig.2(a) corresponds to $n = 2$, $B = 4$ T. The strength of magnetic field is shown near the lines.

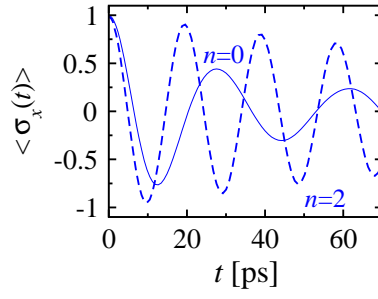


FIG. 3: (Color online) $\langle \sigma_x(t) \rangle$ for a short-range potential ($R_g = 3$ nm) in the GaAs quantum well, with $B = 4$ T. Landau level numbers are shown near the lines.

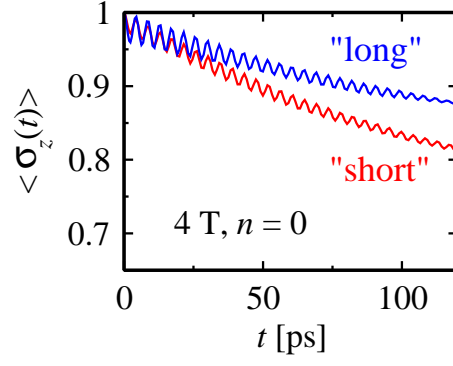


FIG. 4: (Color online) $\langle \sigma_z(t) \rangle$ for long-range and short-range potentials in the $\text{In}_{0.5}\text{Ga}_{0.5}\text{As}$ quantum well.